GEOPHYSICAL RESEARCH LETTERS, VOL. 25, NO. 9, PAGES 1351-1354, MAY 1, 1998

Dynamics of Rocky Mountain lee waves observed during SUCCESS

J. Dean-Day[1], K. R. Chan[2], S. W. Bowen[1], T. P. Bui[2], B. L. Gary[3], and M. J. Mahoney[3]

Abstract. On two days during SUCCESS, the NASA DC-8 flew carefully designed flight tracks to sample wave clouds downstream of the Rocky mountains. Wave morphology was deduced by applying linear perturbation theory to in-situ measurements of the Meteorological Measurement System (MMS) and remotely sensed isentrope profiles of the Micro-wave Temperature Profiler (MTP). Vertical winds from the MMS were consistent with updraft velocities derived from air parcel displacements estimated from the MTP. Derived wave characteristics and cooling rates are useful inputs to cloud microphysics models.

1. Introduction

Mountain waves are generated when the atmosphere is stably stratified, winds are nearly orthogonal to the mountain range, and wind direction is roughly constant with altitude. Lenticular clouds are often formed in the updraft portions of these standing gravity waves when the atmosphere is close to saturation. A case study of stratospheric mountain waves based on ER-2 MMS data was reported by Chan et al. (1993).

The DC-8 MMS, an aircraft-specific instrument developed for SUCCESS (Chan et al., 1998), provides measurements of pressure (p), temperature (T), the 3-d wind (u, v, w), aircraft attitude, position and velocities. The MTP is a passive radiometer, measuring thermal emission from oxygen molecules at 10 elevation angles. In each cycle (15 s), 30 observed brightness temperatures are converted to a temperature profile, T(z), using appropriate retrieval coefficients. T(z) profiles are used to create cross-sections of isentrope (θ) surfaces (Gary, 1989; Denning et al., 1989). The derived profiles of static stability are important in deducing wave behavior.

The MMS and MTP provide simultaneous sampling of high-resolution 3-d winds and horizontal and vertical thermal structure of waves, allowing the study of propagation characteristics as determined from the combined data sets. For each encounter, wave scale, orientation, propagation mode, vertical displacement, and updraft velocity were determined from MMS and MTP data. This is the first time that wave characteristics can be deduced from a single level flight by one aircraft.

2. Analysis

Wave behavior is described by applying linear perturbation theory to a set of momentum, thermodynamic and continuity equations. When applied to MMS and MTP data, many wave characteristics (wavelength, orientation, propagation mode, phase relationships, etc.) can be determined; we follow Clark and Morone (1981) for 3-d hydrostatic waves in a non-rotating atmosphere. To allow density variation (compressibility) without including sound waves, an *anelastic* approximation is used in the continuity equation (Ogura and Phillips, 1962). The waves examined here are hydrostatic in nature, and do not required the non-hydrostatic assumption, applicable to wave scales < 30 km (Klemp and Lilly, 1978).

During wave encounters, MMS data showed strong fluctuations, and most organized relationships were between u and T. For *vertically propagating* waves in the troposphere and lower stratosphere,

$$u' \approx \frac{igk\hat{\omega}}{N^2|\vec{k}^2|}\left(m+\frac{\imath}{\gamma H}\right)\frac{T'}{\overline{T}}$$

where g is gravity, k the zonal wavenumber, $\vec{k}$ the wavenumber vector, m the vertical wavenumber, $\hat{\omega}$ the intrinsic wave frequency, N the Brunt-Väisälä frequency, γ the ratio of specific heats (c_p/c_v), H the atmospheric scale height, u', v' and T' the zonal wind, meridional wind and temperature perturbations induced by the wave, and $\overline{T}$ the mean temperature. Under the same conditions, for *decaying* waves,

$$u' \approx \frac{-gk\hat{\omega}}{N^2\overline{T}|\vec{k}^2|}\left(\frac{1}{N^2}\frac{\partial}{\partial z}N^2+\frac{N^2}{g}+\frac{1}{\gamma H}-\frac{1}{T'}\frac{\partial T'}{\partial z}\right)T'$$

For all gravity waves in an atmosphere where the lapse rate is positive,

$$w' = -\frac{ig\hat{\omega}}{N^2\overline{T}}T'$$

For deep *propagating* waves ($\lambda_z >> H$), u and T will be aligned in phase, while for waves of intermediate depth ($\lambda_z \approx H$), u and T will have a relationship between in phase and in quadrature. For shallow *propagating* waves, the H term vanishes and quadrature phase is predicted. For *decaying* waves, terms involving either H or $\partial T/\partial z$ dominate the solution, As a

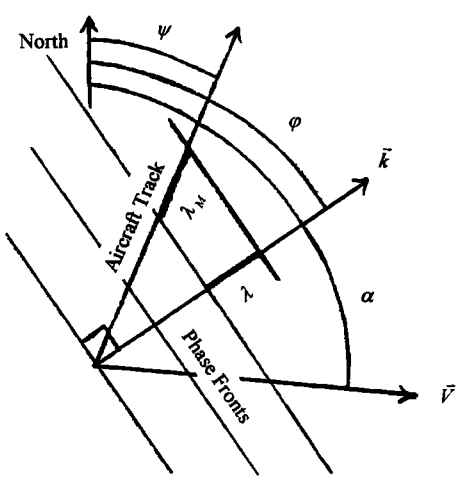

Figure 1. A schematic of the wind angle α, aircraft track angle Ψ, and wave vector angle φ for an arbitrary level-flight leg.

[1]San Jose State University, San Jose, California
[2]NASA, Ames Research Center, Moffett Field, California
[3]Jet Propulsion Laboratory, Pasadena, California

Paper number 98GL01004.
0094-8534/98/98GL-01004$05.00

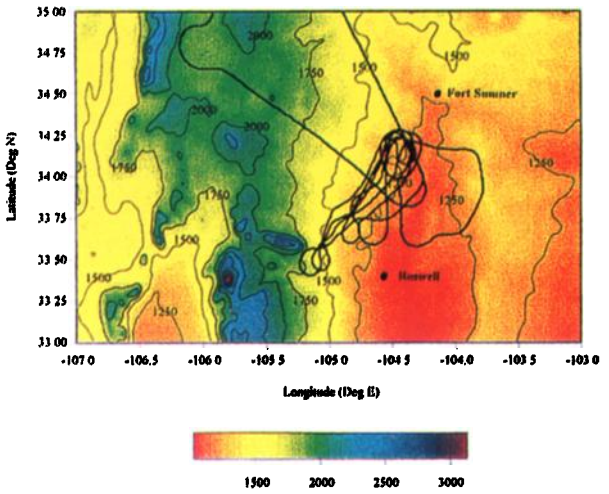

Figure 2. Topographic contour map (250 m contour interval) covering a portion of New Mexico where the 960430 wave encounter occurred. The DC-8 flight path is outlined in black.

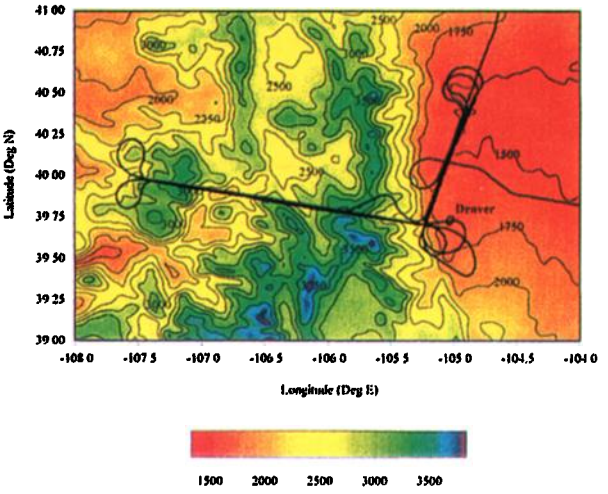

Figure 4. Topographic contour map (250 m contour interval) covering a portion of Colorado where the 960502 wave cloud encounter occurred. The DC-8 flight path is outlined in black.

result, u and T are in phase regardless of the wave depth; w and T are in quadrature phase under all circumstances.

Figure 1 shows the wind angle α, aircraft track angle Ψ, and wave vector angle φ for an arbitrary level flight leg. These angles form relationships between aircraft measured (λ_{AI}) and actual (λ) horizontal wavelengths, and between the wind velocity $(\vec{V})$ with its component across the wave fronts $(\vec{u})$ These are used in defining the intrinsic frequency (Cadet and Tietelbaum, 1979),

$$\hat{\omega} = \omega - \vec{k} \bullet \vec{u}$$

where ω is the wave frequency with respect to Earth. For stationary waves ($\omega = 0$), replacing the right-hand side with measured quantities yields,

$$\hat{\omega} = \frac{-2\pi\sqrt{\overline{u}^2 + \overline{v}^2}\cos(\varphi - \alpha)}{\lambda_{AI}\cos(\varphi - \psi)}$$

Since the equation has two unknowns ($\hat{\omega}$ and φ), it is necessary to sample the same wave packet, at nearly the same time, location, and altitude at two distinct (non-parallel) track angles. It is assumed that the waves share a common orientation within a field of horizontally homogeneous winds. While hydrostatic waves generated by an isolated peak have exhibited parabolic phase surfaces (Smith, 1980), we contend that waves generated by a long ridge will be approximately planar. Equations for the two flight tracks are given by,

$$\lambda_{AI1}\cos(\varphi - \psi_1)\hat{\omega} + 2\pi\sqrt{\overline{u}^2 + \overline{v}^2}\cos(\varphi - \alpha) = 0$$

$$\lambda_{AI2}\cos(\varphi - \psi_2)\hat{\omega} + 2\pi\sqrt{\overline{u}^2 + \overline{v}^2}\cos(\varphi - \alpha) = 0$$

Combining the equations and eliminating the common term, we solved for φ with a Newton-Raphson root finder. This solution is then applied to determine the intrinsic frequency using data from *either* track. Once wave orientation is known, wavelength and propagation characteristics can be deduced. We study only medium to large waves causing T fluctuations greater than ≈ 0.5 K. Depending on specific waves sampled, the minimum wavelength may vary from 5 to 25 km.

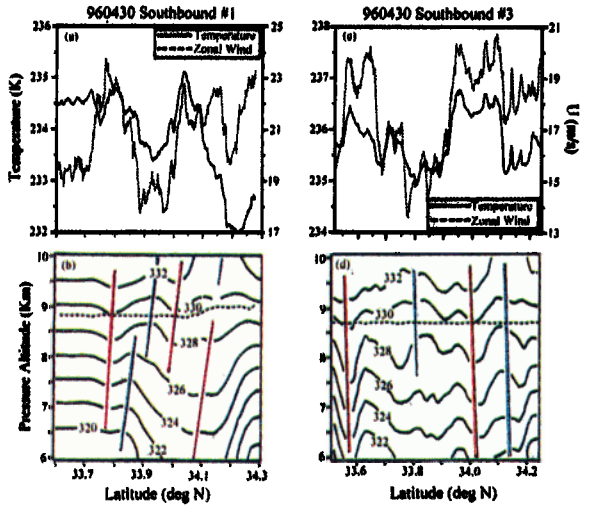

Figure 3. Temperature (T) and zonal wind (u) from the MMS and the isentropic profile from the MTP during the first southbound pass (**a** and **b**) and the third pass (**c** and **d**) through the 960430 mountain wave event. Cool (warm) displacements of isentropes are indicated by blue (red) lines. The DC-8 flight tracks (heavy dotted lines) are outlined on the isentropic profiles (**b** and **d**).

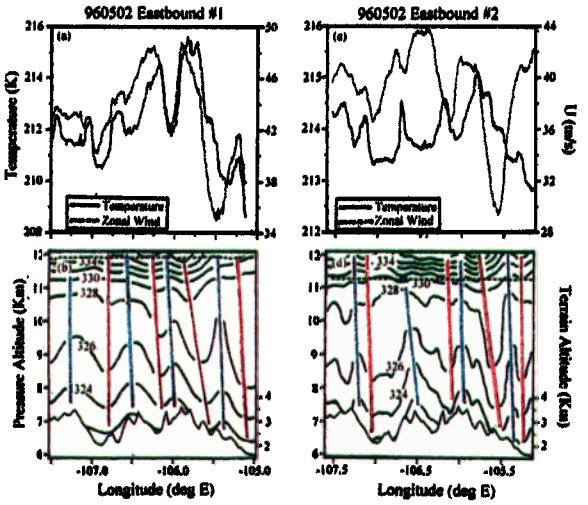

Figure 5. Temperature (T) and zonal wind (u) from the MMS and the isentropic profile from the MTP during the first (**a** and **b**) and the second (**c** and **d**) eastbound passes through the 960502 mountain wave event. Isentropic displacements and the DC-8 flight tracks are denoted as per Figure 3.

3. Results

3A. 960430 Wave Encounter near Fort Sumner, New Mexico

With aircraft velocity at ≈ 230 $m\ s^{-1}$, the DC-8 was flown into the wave region at 11 *km* from the northwest, passing close to a ridge of mountains just east of Albuquerque, NM. At this altitude, no waves were observed. The aircraft descended to 8.5-8.8 *km*, and a number of passes (100 km) were made on N-S and SW-NE headings 100 *km* downstream from the major topographic features (Figure 2). Some flight legs traversed wave clouds, while others showed little or no evidence of cloud formation.

Five tracks were chosen to study the wave dynamics: four nearly coincident legs between 33.4°N, 105.2°W and 34.2°N, 104.4°W, and a fifth quasi-westward leg (45 km) along 34.2°N between 104.4°W and 103.9°W. The coincident tracks were oriented from SW through NE, ≈ 30° off the meridian.

MMS data show considerable variability on a variety of scales (Figures 3a and 3c). Peak-to-peak amplitudes are 5 $m\ s^{-1}$ for u and v, 3-4 $m\ s^{-1}$ for w (not plotted) and ≈ 1-2 K for T. Although T dips toward the end of the first southbound leg, due to the effect of thermal stratification (Figure 3a), close examination of u and T during two of the traverses show a persistent pattern of positively correlated troughs and ridges.

Locations of MMS troughs and ridges (Figures 3a and 3c) generally correspond to the θ–surface undulations observed by the MTP (Figures 3b and 3d). The DC-8 flew through the waves between the 328 K and 330 K isentropes on both legs, where the peak-to-peak undulation amplitude was 400-500 *m*. Some undulations show diminishing amplitude with height. The phase surfaces are very steep, suggesting the vertical wavelength is at least as deep as the scale height (≈ 6.3 km).

During ≈ 35 minutes between the first and third passes through this wave region, the largest scale features in both MMS and MTP data shift to the south by 0.1-0.2° latitude. If the wave vector were parallel to the flight track, this would correspond to a maximum phase speed of ≈ 7 $m\ s^{-1}$. Since v does not closely correlate with features seen in T, the wave vector is aligned quasi-zonally, As such, the waves are quasi-stationary. The positive correlation between u and T, the corresponding features in MMS and MTP data, and the small phase speed are all indicative of orographic waves.

Using both MMS and MTP data, we solve for the wave orientation angle and intrinsic frequency. Background conditions and results are summarized in Table 1. The wave phase planes are aligned only 11° off the direction of the flight tracks, reducing the phase speed to only 1.3 $m\ s^{-1}$. Based on wave characteristics, air will flow through the standing waves at 21.5 $m\ s^{-1}$, and pass from trough to crest in 215 s^{-1}. Combining a temperature departure from equilibrium of ~ 0.8 K with the lapse rate $\Gamma = 6.3\ K\ km^{-1}$, (MTP data; $N = 0.012\ s^{-1}$) yields a vertical displacement from equilibrium of 230 m. If the vertical velocity is sinusoidal, it yields $w_{max} = 3.0\ m\ s^{-1}$. These waves meet the decay criterion $(\hat{\omega} > N)$ which serves to explain why they could not be sampled on the inbound and outbound flight legs in this region.

Table 1 The 960430 Mountain Wave Encounter

Input Parameter	Result from Wave Equations
$\overline{u}$ (m s^{-1})	20.0
$\overline{v}$ (m s^{-1})	-8.0
λ_{A1} (km)	50.0
λ_{A2} (km)	9.5
ψ_1 (deg)	30.0
ψ_2 (deg)	96.5
φ (deg)	109.0
λ (km)	9.3
$\lvert\hat{\omega}\rvert$ (s^{-1})	0.0146
N (s^{-1})	0.010

Table 2 The 960502 Mountain Wave Encounter

Input Parameter	Result*	Result*
Z_p (km)	11.8	11.2
$\overline{u}$ (m s^{-1})	42.0	38.0
$\overline{v}$ (m s^{-1})	-4.0	-2.0
λ_{A1} (km)	36.3 ± 4.3	37.5 ± 4.3
λ_{A2} (km)	56.2 ± 2.3	43.0 ± 3.5
ψ_1 (deg)	100.0	100.0
ψ_2 (deg)	19.0	19.0
φ (deg)	73.6 ± 5.0	64.1 ±6.5
λ (km)	32.5 ± 2.5	30.4 ± 1.0
$\lvert\hat{\omega}\rvert$ (s^{-1})	0.00756 ± 0.001	0.00689±0.0007

* Wave equations are solved for each flight altitude because of differences in the mean wind.

3B. 960502 Wave Encounter over the Colorado Rockies

On 960502, the DC-8 flew a series of W-E and SSW-NNE flight tracks, intersecting above Denver, CO (Figure 4), nearly parallel and perpendicular to the prevailing wind. Two westbound and two eastbound tracks were coincident, extending across several sets of ridges in clear air (≈ 200 *km*) westward from Denver (39.7°N, 105.2°W) to upstream of Flat Tops Wilderness (40.0°N, 107.5°W). Two northbound and three southbound tracks (90 *km*) were coincident but downstream of the mountains, overflying the plains in wave clouds north of Denver to Greeley and Fort Collins (40.5°N, 104.9°W). The last pair of flight tracks (after 74,500 s UT) were at 11.2 *km*, whereas the earlier passes were at 11.8 *km*. MMS winds (Figures 5a and 5c) and MTP static stability data (Figures 5b and 5d) were greater on the upper flight tracks. The tropopause was located near or below the 11.2 *km* level.

Waves were evident in the MMS data along all legs. As many as six peaks and valleys are observed in u and T data as the DC-8 flew cross-mountain tracks, corresponding to the vertical displacement pattern of the MTP isentropes. Positions of the major features show little or no movement with time.

Along higher flight tracks, u and T show an in-phase relationship (Figure 5a), while on lower flight tracks, u and T are in quadrature phase (Figure 5c). Below both flight tracks, MTP data show wave-growth and slight upstream wave-tilt with height between θ = 322 K and θ = 326 K. Oscillations in T align with features in the θ-contours. Over the foothills west of Denver, θ-displacements at the 9-10 km level exceeded 2 *km* (where $N = 0.004\ s^{-1}$, not plotted). Vertical displacement of the θ-contours at flight level is generally 300-600 m.

Wave equations were solved for a common set of flight track orientations, but with different wind velocities for each altitude. Background inputs included data from multiple parallel tracks averaged over time; inputs and results are summarized in Table 2. At both altitudes, the derived wave has a length of 30-32 *km* oriented ≈ 70° from north. Given the wind direction as stated, it will take 425 s for air to pass through the wave from trough to crest. Using $N = 0.016\ s^{-1}$ ($\Gamma = 4.3\ K\ km^{-1}$,) and $T' = 0.6\ K$ (measured westward from the crest of the

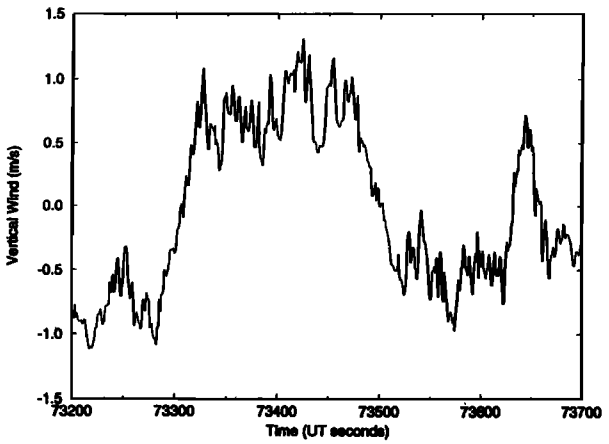

Figure 6. Vertical wind (mean removed) for a northbound flight leg to the lee of the Rockies.

Rockies) yields a vertical displacement of ~ 110 *m* from equilibrium and w_{max} = 0.7 *m* s^{-1}. The intrinsic frequency indicates an upward propagating wave. This is consistent with the observed *u-T* phase relationship only for a very deep wave, as indicated by the steep slope of the phase planes.

This particular wave, however, underestimates the updraft velocity measured on N-S flight legs (Figure 6). The dip in *T* at the east end of the longitudinal tracks, as well as the downward sag in *θ(z)* cross-sections below the flight tracks, suggest the presence of a longer wave. A broad peak in *T* occurs at 105.8°W, with a corresponding trough at about 107.0°W. The presence of warm air above high peaks suggests the presence of a second wave formed by the mountain ranges as a whole. The phase reversal at flight altitudes suggests that the vertical wavelength is nearly twice the tropopause height.

The wavelength was estimated to be 170 *km*. With ΔT = 1.2 *K*, it yields a vertical displacement from the steady state of 220 *m* , comparable to the total displacement observed by the MTP. At 40 *m* s^{-1}, ≈ 2100 s are required for air to pass from trough to crest, yielding w_{max} = 0.3 *m* s^{-1} and a total updraft of 1.0 *m* s^{-1}. This reflects the observed w more accurately.

4. Conclusion

Dominant features of the 960430 and 960502 mountain waves have been deduced from the MMS (T, u, v, w) and MTP (isentropic and stability profile) observations. Data from one instrument are consistent with the other in terms of characterizing the nature of encountered waves. Using linear theory, flight-track geometry and MMS/MTP measurements, the intrinsic frequency and orientation of each dominant wave were deduced. Wavelength, air-parcel transit time, and propagation characteristics were also determined. Waves over New Mexico were found to be decaying, while waves over Colorado were formed by at least two superimposed propagating waves.

The 960430 wave over New Mexico was shorter in length (9.3 *km*) than those over the Colorado Rockies and plains on 960502 (30-32 *km* and ≈ 170 *km*). Despite larger size and stronger *T*, the updraft in the Colorado wave was less than half of that in the New Mexico wave. Larger mountain waves may have weaker updrafts, but the integrated effect over time can produce larger displacement of air parcels. Smaller mountain waves may cause fast (< 60 s) nucleation and growth of ice crystals to an equilibrium concentration and size distribution. In both wave encounters, the *T* signal in MMS data, combined with the background static stability, yield vertical displacements consistent with those from the MTP isentropes.

To study the nucleation and growth of ice crystals in cirrus clouds, it may be useful to characterize these processes within larger orographic waves such as the one observed on 960502. There may be regions near the tropopause, *upstream* of mountain ranges, where large-scale waves with gentle vertical motions propagate into an advecting field of highly moist air. Such areas may be devoid of the smaller waves and their associated strong vertical motion field. As such, ice nucleation and growth processes may resemble that which take place in cirrus clouds, taking place in an environment which can be readily characterized.

5. References

Cadet, D., and H. Teitelbaum, Observational evidence of internal inertia-gravity waves in the tropical stratosphere, *J. Atmos. Sci., 36*, 892-906, 1979.

Chan, K. R., L. Pfister, T. P. Bui, S. W. Bowen, J. Dean-Day, B. L. Gary, D. W. Fahey, K. K. Kelly, C. R. Webster, and R. D. May, A case study of the mountain lee wave event of January 6, 1992, *Geophys. Res. Lett., 20*, 2551-2554, 1993.

Chan, K. R., J. Dean-Day, S. W. Bowen, and T. P. Bui, Observation of turbulence by the DC-8 Meteorological Measurement System, submitted to *Geophys. Res. Lett*, this issue, 1998.

Clark, J. H. E., and L. T. Morone, Mesospheric heating due to convectively excited gravity waves - a case study, *Mon. Wea. Rev., 109*, 990-1001, 1981.

Denning, R. F., S. L. Guidero, G. S. Parks, and B. L. Gary, Instrument description of the microwave temperature profiler, *J. Geophys. Res., 94*, 16757-16765, 1989.

Gary, B. L., Observational results using the microwave temperature profiler during the Airborne Antarctic Ozone Experiment, *J. Geophys. Res., 94*, 11223-11231, 1989.

Klemp, J. B., and D. K. Lilly, Numerical simulations of hydrostatic mountain waves, *J. Atmos. Sci., 35*, 78-107, 1978.

Ogura, Y., and N. A. Phillips, Scale analysis of deep and shallow convection in the atmosphere, *J. Atmos. Sci., 19*, 173-179, 1962.

Smith, R. B., Linear theory of stratified hydrostatic flow past an isolated mountain, *Tellus, 32*, 348-364, 1980.

T. P. Bui and K. R. Chan, NASA, Ames Research Center, M.S. 245-5, Moffett Field, CA 94035-1000. (email: rchan@mail.arc.nasa.gov)

S. W. Bowen and J. Dean-Day, San Jose State University, San Jose, CA 95192. (email: day@mms.arc.nasa.gov)

B. L. Gary and M. J. Mahoney, NASA, Jet Propulsion Laboratory, M. S. T-1182, Pasadena, CA 91109-8099. (email: bgary@jpl.nasa.gov)

(Received July 1, 1997; revised January 23, 1998; accepted March 12, 1998.)